Simulation-based Assesment of Quality of Service in UAV-assisted mmWave System in Crowded Area

Danil S.Vasiliev, Albert Abilov, Irina A. Kaysina
Izhevsk State Technical Univestity
Izhevsk, Russia
{danil.s.vasilyev, albert.abilov, irina.kaysina}@istu.ru

Daniil S. Meitis
CJSC NPO Telecom
Izhevsk, Russia
dsmejtis@npotelecom.ru

***Abstract*—In this paper, we assess the applicability of millimeter wave (mmWave) system with mmWave-enabled unmanned aerial vehicle (UAV-BS) in crowded area using the NS-3 simulation tool. We simulate the transmission at 28GHz between the base station (BS) and the user terminal (UT). The BS and the UT are located in opposite corners, and the UAV is located in the middle of the square. We measure end-to-end quality of service metrics at the remote host for scenarios with UAV and without it for various densities of blockers. The relaying using UAV-BS demonstrated the gain in goodput metric up to 80% for the scenario with high blockage. The remarkable properties of mmWave system are considered using 100Mbps UDP stream from the UT to the remote host.**

I. Introduction

The demand for mobile communication facilities is expected to increase on a large scale as number of Internet-connected things grows, and, as a consequence, industry and academia are working to anticipate this situation, for example, with help of 3rd Generation Partnership Project (3GPP) New Radio (NR) [1]. They are experimenting with a millimetre wave (mmWave) systems which utilize extremely high frequencies (EHF) over 24 GHz [2-5]. These systems use antenna arrays and beamforming techniques to maintain high directionality of beams between user terminals (UT) and base stations (BS) in cellular network. A throughput of several gigabits per second is reachable in the mmWave system, and it is the essential component of next generation of mobile communications (5G) at physical layer. It will also influence all protocols at higher layers of OSI model [6]. In the paper, we would like to present the assessment of end-to-end Quality of Service (QoS) in mmWave system with the mmWave-enabled unmanned aerial vehicle (UAV).

At this time many problems of the mmWave system are being considered: how to cope with high variability of channel [2], how to make use of the system in areas with human blockage [7], how to implement multi-connectivity [8], what applications of such system are promising [9]. The communication possibilities of various beamforming techniques are also being investigated [2].

The attenuation during rainstorms began to rise noticeably above about 10 GHz. Obstacles between a receiver and a transmitter could cause non-line-of-sight condition, and fading range is great challenge.

Transmission by means of mmWaves offers problems as well as advantages, because these systems make use of an extremely high frequencies and particular ambiguous transmission medium – the air of crowded city streets, suburban and rural areas.

Engineers made considerable use of millimeter equipment for point-to-point communications. Today, researchers make use of mmWave links to transmit data between base stations (BS) and mobile user terminals (UT). Researchers are working to understand the transmission characteristics of mmWave systems. They are studying the propagation of 28GHz, 38GHz, 60 GHz, and 73GHz in different scenarios and developed many essentials analytical models at physical layer [2]. They tended to establish new requirements for higher layer protocols and transmission techniques for communication in new range of frequencies. New applications are also considered, e.g., the railroad-operated mmWave communication system is proposed in [10]. This system will supplement and perhaps eventually replace GSM and LTE facilities.

LTE systems are capable of transmitting a lot of data, but studies comparing the desired throughput on microwaves and on mmWaves showed that higher frequencies might be only way to give adequate QoS for new applications, e.g. massive Internet of Things. There several reasons for moving fast in the mmWave field: one of the most important was that throughput of LTE systems was at the threshold in metropolis areas (e.g., New York, London, and Moscow). Many companies in telecommunication industry are looking forward to rapid expansion in this new field.

The remainder of this paper is organized as follows: Section II, overview of UAV-assisted mmWave systems, Section III, system model; Section IV, description of chosen simulation scenario; Section V, results; Section VI, conclusion.

II. UAV-assisted mmWave System

Modern communication systems could be operated by aerial nodes, e.g., copters or fixed-wing drones [11]. Researchers investigated the ability for UAVs to be served using LTE network deployments with BS antennas targeting terrestrial coverage in [12].

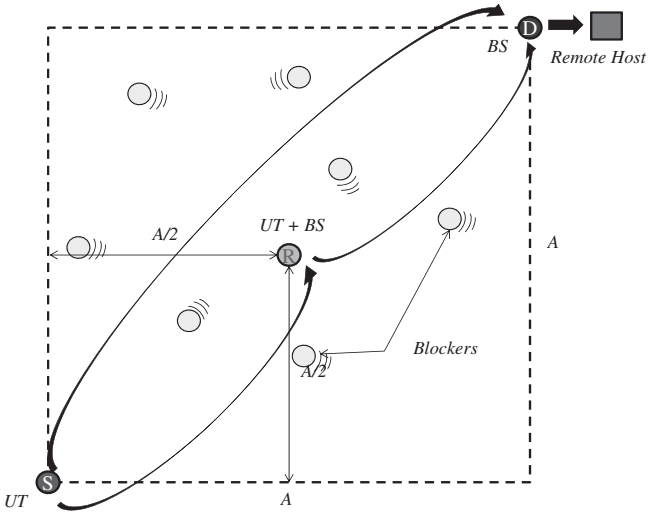

Fig. 1. Top-view of simulated unmanned aerial vehicle (UAV)-assisted mmWave system. Black arrows show UDP streams from the user terminal (UT) to the remote host. Human-size blockers are moving in random walk manner in the square area with side *A*.

Mobile relay was proposed in LTE systems [13]. It is obvious this technique has emerged from technologies of previous generation to become a vital part of 5G communication systems [14]. Performance-wise, the mmWave system, being more vulnerable to the blockage, should provide greater throughput than the LTE system. Furthermore, it will carry more data and can be expanded more readily with help of UAVs [15], [16].

A scenario where an unmanned aerial vehicle BS (UAV-BS) is deployed to provide coverage over a large stadium/concert with thousands of mobile users distributed on the ground is considered in [17].

A novel framework that leverages user-centric information, such as content request distribution and mobility patterns, to effectively deploy cache-enabled UAVs while maximizing the users' quality of experience (QoE) using a minimum total transmit power of the UAVs is considered in [18].

Random heights of drones and UT and the highly directional nature of mmWave links are considered in [19].

We analyze the mmWave system that consists of the UT, the BS, and the UAV-BS (Fig.1 and Fig.2). MmWave-enabled UAV is combined UT+BS entity. In the paper we consider the 28GHz band that offers many advantages, such as deployment of antenna arrays and high throughput. The practical length of a hop is determined by the height of the antenna support (or UAV altitude), terrain, transmitter power. Line-of-sight (LOS) and non-line-of-sight (NLOS) conditions are not good except for very short hops. We consider using of an UAV to improve QoS metrics in transmission in crowded area where LOS path is blocked by human-size obstacles. We consider the UAV-BS as stationary BS serving only one UT and connected by mmWave link to traditional BS.

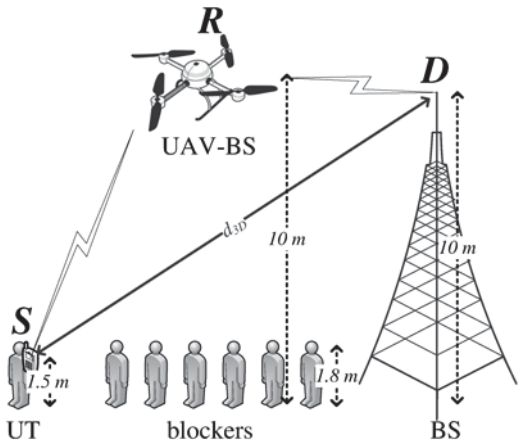

Fig. 2. User terminal (UT), base station (BS), and unmanned aerial vehicle

The system, that applies drones to communication by mmWaves, gives many opportunities and challenges for the low and high layer protocols and plays an important part in the development of effective mmWave communications.

Beams at EHF frequencies will operate between the UT and the UAV-BS, the UAV-BS and the BS (Fig.2). It is expected that, ultimately, mmWave beams will be delivered with more efficiency using the UAV-BS.

III. MmWave System Model

The advances in analytical modeling of mmWave technology that had been made were vitally important in the big push on system level simulations. One of several developments carried to successful completion by researchers was LTE-like 5G cellular network implemented in NS-3 simulation tool. This simulation environment utilizes existing analytical models for path loss, spatial consistency (Procedure A), and small scale fading.

We assess end-to-end efficiency of mmWave system using NS-3 simulation tool [20], [21], [22]. Simulated scenario is presented in Fig.1 and Fig.2. We consider the system that consists of the BS, the UT, and the UAV-BS. During the simulation the UAV-BS is connected to both UT and BS by mmWave links. The BS treats the UAV-BS as common UT. At other hand, the UT considers the BS and the UAV-BS as two different base stations.

We use `mmwave-simple-epc.cc` script from examples on `github.com/nyuwireless-unipd/mmwave` to simulate transmission of packets from the UT to the remote host in Internet through the BS and Evolved Packet Core (EPC). Both BS and UAV-BS are connected to PGW/SGW and further to Internet. MmWave link between the UAV-BS and the BS is implemented as a link between flying UT and the BS (Fig.3). This flying UT is connected to the flying BS by internal relay interface. This interface makes UAV-BS transparent for packets from the UT to the BS and vice versa. MmWave devices use time-division duplex (TDD) scheme.

The simulation provides the practical gain of the UAV-assisted LTE-like mmWave cellular network. Simulation parameters are presented in the Table I (Fig. 1 and Fig.2). We modeled our nodes in Rural Macrocell (RMa) scenario of 3GPP Propagation Model with the NS–3 buildings module. 3GPP channel model is recommended for QoS estimation in mmWave systems. Currently, RMa scenario is validated only for frequencies up to 7GHz [23],[24], but it is a realistic scenario for UAV-assisted mmWave system. During the simulation we consider two general causes for low end-to-end QoS in mmWave systems: the path loss and the blockage [25].

`MmWave3gppBuildingPropagationLossModel` is used to show negative effect of the blockage in and the path loss in mmWave system. Class diagram is presented in Fig.3.

A. The Path Loss

The path loss could be described by analytical 3GPP signal propagation model. We consider rural macrocell scenario (RMa) that has many constrains on minimal and maximal heights of the BS and the UT. The applicable frequency range of the path loss (*PL*) formula is $0.8 < fc < f_H$ GHz, where f_H = 30 GHz for RMa [24]. It is noted that RMa path loss model for >7 GHz is validated based on a single measurement campaign conducted at 24 GHz. In our simulation packets are transmitted at the central frequency of 28 GHz.

We chose values from the applicability ranges to model the system with the UAV-BS using these equations. The UAV-BS in our simulation is the combination of the flying UT and flying BS. The recommended height of UT h_{UT} is from 1 to 10 meters. The possible height of the BS h_{BS} is from 10 to 150 meters. Chosen altitude of the UAV-BS h_R is 10 meters.

Following *PL* expressions are used for the line-of-sight (LOS) path loss:

$$PL_{RMa\text{-}LOS}=PL_1,\ 10m \le d_{2D} \le d_{BP}$$

$$PL_{RMa\text{-}LOS}=PL_2,\ d_{BP} \le d_{2D} \le 10km$$

$$PL_1=20\log_{10}(40\pi \cdot d_{3D} \cdot f_c / 3)+\min(0.03h^{1.72},10)\log_{10}(d_{3D})-\min(0.044h^{1.72},14.77)+0.002\log_{10}(h)d_{3D} \quad (1)$$

$$PL_2=PL_1(d_{BP})+40\log_{10}(d_{3D} / d_{BP})$$

where d_{2D} and d_{3D} are distances between the UT and the BS in 2D and 3D (fig.2), d_{BP} *is* a breakpoint distance, h – average building height (5 meters by default), W – average street width (20 meters by default).

If the channel is in non-line-of-sight (NLOS) condition, the path loss is described by the following equations:

$$PL_{RMa\text{-}NLOS}=\max(PL_{RMa\text{-}LOS},\ PL'_{RMa\text{-}NLOS}) \quad for\ 10m \le d_{2D} \le 5km$$

$$PL'_{RMa\text{-}NLOS}=161.04-7.1\log_{10}(W)+7.5\log_{10}(h)-(24.37-3.7(h / h_{BS})^2)\log_{10}(h_{BS})+(43.42-3.1\log_{10}(h_{BS}))(\log10(d_{3D})-3)+20\log_{10}(f_c)-(3.2(\log_{10}(11.75h_{UT}))^2-4.97) \quad (2)$$

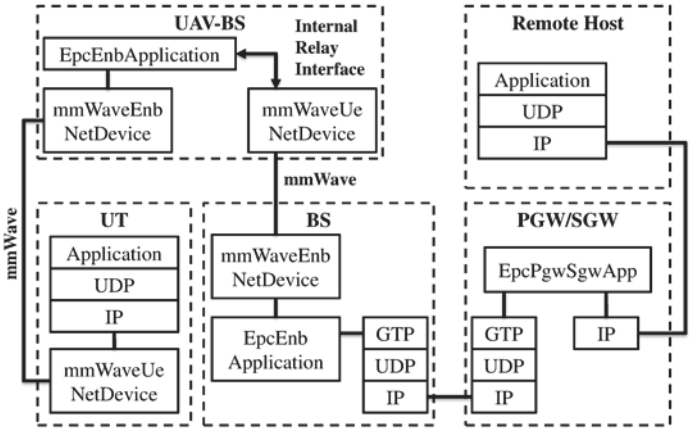

Fig. 3. Class diagram for UAV-assisted mmWave system model

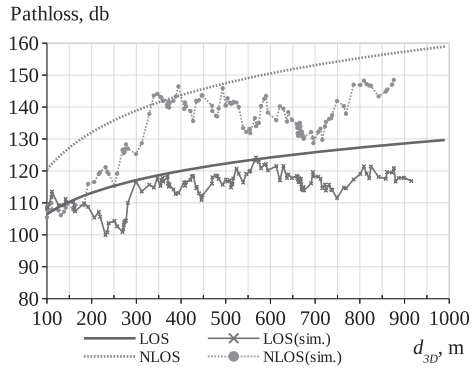

Fig. 4. The dependence between the path loss and the distance d_{3D} (between the BS and the UT)

In Fig.4 path loss values in our simulation are presented for various distances d_{3D} between the BS and the UT. Lines without markers present analytical values based on equations (1) and (2) for the path loss. Lines with markers present instant path loss values from the simulation in NS-3. In the simulation we manually set LOS and NLOS channel conditions, and moved the UT from the BS with the speed of 10 meters per second. Distance d_{3D} between them changed from 100 to 900 meters.

TABLE I. SIMULATION PARAMETERS

Parameter Name	Value
Center Frequency, GHz	28
UT Antenna number	16
BS antenna number	48
Side A, meters	[100..1000]
Transport Layer	UDP
Source datarate, Mbps	≤100
Tx Power, dBm	20
Small Scale Fading	Enabled
UT height h_{UT}, meter	1.5
Blocker height h_{block}, meter	1.8
Blocker width, meter	0.5
Blocker density, ρ_{block} ,1/m^2/	[0.001…0.1]
Blocker mobility model	Random Walk
Blocker velocity, meters per second	2
Simulation time, seconds	60
BS height h_{BS}, meters	10
UAV-BS altitude h_R, meters	10

B. The blockage

In mmWave system signals are easily blocked by obstacles. In our simulation we assess the blockage from small moving obstacles. Each blocker is a cuboid with sides 0.5*0.5*1.8 meters (width*depth*height). The cuboid is rude representation of human body that could block mmWave signals. We model the square area with [90…9000] humans to make propagation of signal harder for direct route between the BS and the UT. Blockers are moving in random walk manner with velocity of 2 meters per second. Such model could describe people in a stadium, a park, or music festival.

We analyze the square area with side A from 100 to 1000 meters. The relationship between the number of blockers and the size of the area is the blocker density ρ_{block} value. We define the number of blockers N_{block} during the simulation using the equation:

$$N_{block} = \rho_{block} * (D_{max} - D_{min})^2, \quad (3)$$

where ρ_{block} – the density of blockers in the area in $1/m^2$, D_{max} – the maximal distance from the BS in meters (it is similar to side A by default), D_{min} – the minimal distance from the BS in meters (10 meters by default).

IV. Simulated Scenarios

We compare two approaches to data delivery in mmWave systems (with and without the UAV-BS) using NS-3 simulation tool. Channels between nodes are modeled based on 3GPP propagation model at center frequency of 28 GHz. The UAV-BS is used to relay packets from the UT to the BS. We consider two cases: source-destination (SD) and source-relay-destination (SRD).

A. Source-Destination

In the source-destination (*SD)* case the UT is the source *S*, and the BS is the destination *D*. The source and the destination are stationary. The UT is located in the point with coordinates (A, A, 1.5), where A – the side of the square area. The BS is located in the point with coordinates (0, 0, 10). The application at the UT sends data to the remote host in Internet through the local BS. Each packet is transmitted from the UT to the BS with help of mmWave system and then routed by the PGW/SGW entity to Internet.

B. Source-Relay-Destination

In the source-relay-destination (*SRD)* case the UT is the source *S*, the BS is the destination *D,* and the relay *R* is the intermediate UAV-BS in the center of the area. In SRD case the UAV-BS could transparently relay packets from the UT to the BS. The UT, the BS, and the UAV-BS are stationary and located in the points with coordinates (A, A, 1.5), (0, 0, 10), and (A/2, A/2, 10), respectively.

The application at the UT sends data to the remote host in Internet, and each packet is transmitted from the UT to the UAV-BS and then from the UAV-BS to the BS with help of mmWave links. At the BS packets are routed to Internet through the PGW/SGW entity.

C. Quality of Service metrics

We evaluate the efficiency of source–relay–destination (SRD) scheme in mmWave system with UAV-BS using quality of service (QoS) metrics: average goodput and goodput gain. Average goodput ($Goodput_{ave}$) is all UDP payload received by the remote host during the simulation divided by the simulation time:

$$Goodput_{ave} = buf * 8 / T, \quad (4)$$

where *buf* – the size of receiving buffer in bytes, T – simulation time in seconds.

We calculated the goodput gain ($G_{goodput}$) as:

$$G_{goodput} = (Goodput_{SRD} / Goodput_{SD}) - 1, \quad (5)$$

where $Goodput_{SRD}$ – average goodput for source–relay–destination (SRD) case, $Goodput_{SD}$ – average goodput for source–destination (SD) case.

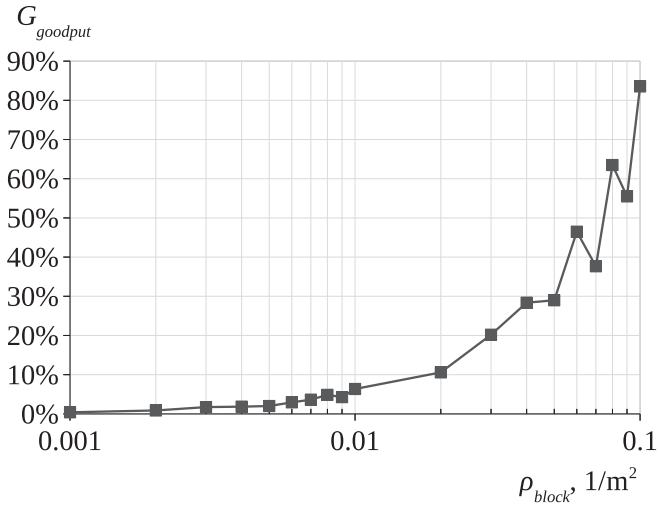

Fig. 5. The goodput gain ($G_{goodput}$) for various blocker densities ρ_{block} in scenario with A=300 meters and the UAV-BS in the center

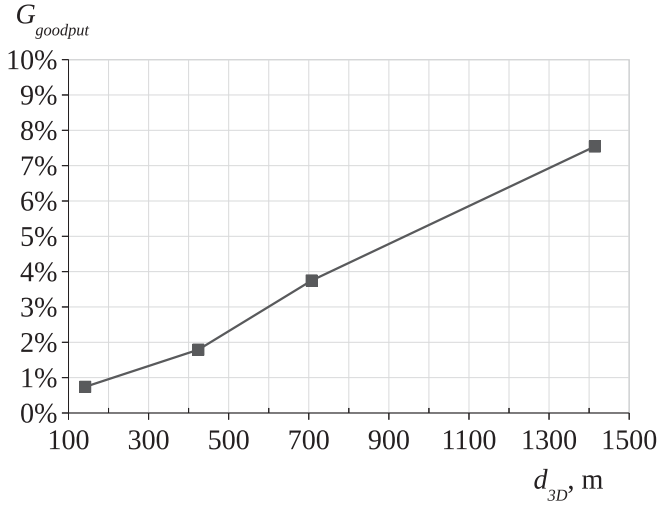

Fig. 6. The goodput gain ($G_{goodput}$) for various distances d_{3D} in scenario with the UAV-BS in the center

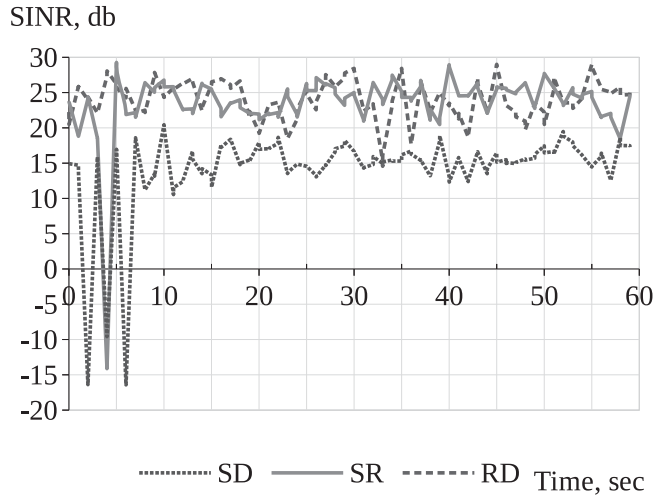

Fig. 7. SINR values for SD, SR, and RD channels (ρ_{block}=0.004, A = 300)

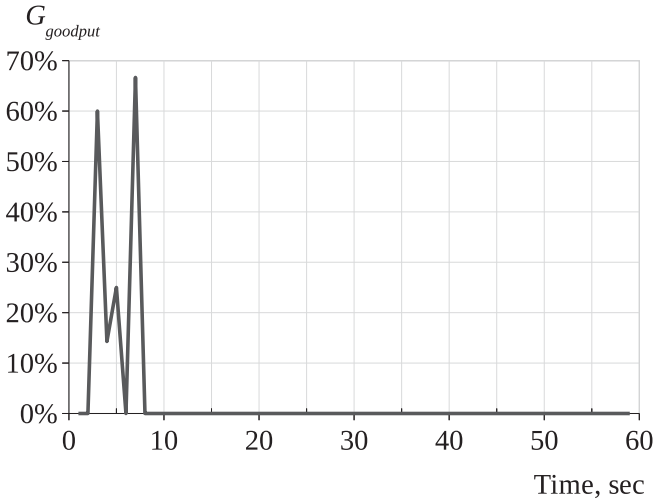

Fig. 8. The goodput gain $G_{goodput}$ during the simulation (ρ_{block}=0.004, A = 300)

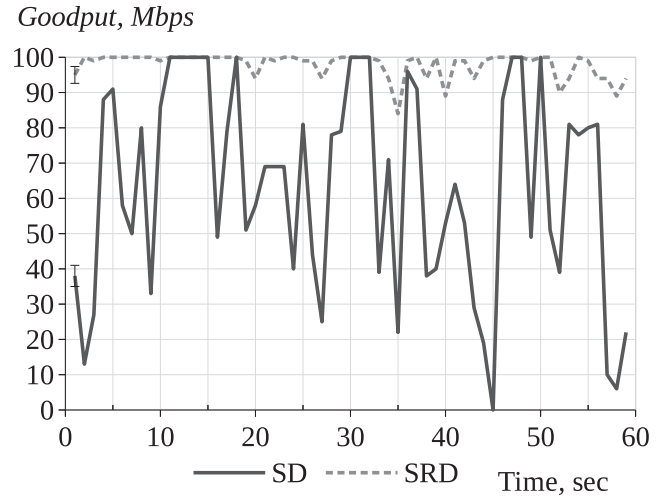

Fig. 9. The example of goodput values during the simulation with high blockage (ρ_{block}=0.04, A = 300): SD – direct transmission from the UT to the BS; SRD – relaying from the UT to the BS with help of the UAV-BS.

We calculated QoS metrics for each case separately: with UAV-BS (SRD case) and without it (SD case). We measured these metrics for data rates 10 Mbps and 100 Mbps and blocker densities from 0.001 to 0.1 blocker per m^2. Fifty runs for each simulated point were performed. The duration of each run was 60 seconds.

V. Results

In simulated cases end-to-end Quality of Service (QoS) metrics depend on physical layer due to negative effect from the path loss and the blockage. The effect of path loss is greater with greater distance between the UT and the BS. The effect of the blockage is greater with higher blocker densitiy ρ_{block}.

Main results are demonstrated in Fig.5 and Fig.6. In Fig.5 the relationship of the goodput gain and blocker density is presented. The side A was 300 meters during all simulation runs, and the UAV-BS was located in the middle of the area. Blocker density of 0.1 blocker/m^2 defines 8410 blockers for the square area with the side A=300. Higher blocker density leads to greater $G_{goodput}$. SRD case gives better average goodput for all measured points. The highest gain of 83% was achieved for the density of 0.1 blocker/m^2. The lowest gain of 0% was at the density of 0.001 blocker/m^2. This relationship could be linearly approximated by the method of least squares as:

$$G_{goodput} = 7.17 * \rho_{block} - 0.006, \quad (6)$$

According to the approximation (6) higher densities will cause even greater gain for SRD case. Such gain is caused by the outages due to the blockage by moving obstacles.

In Fig.6 we demonstrate the dependence of the gain $G_{goodput}$ on the distance d_{3D} between the UT and the BS. Higher distance d_{3D} leads to higher gain for SRD case. For example, the gain for scenario with A=100 meters and d_{3D}≈141 meters is lower than 1%. This distance is too small to demonstrate any gain of relaying through the UAV-BS. But the gain is 7.5% for the same blocker density when A=1000 meters and d_{3D}≈1414 meters.

Fig.7 and Fig.8 illustrate the dependence of end-to-end QoS metric $G_{goodput}$ on physical layer metric SINR. In Fig.7 the SINR for the channel SD between the UT and the BS is around 15db. SINR values for transmission through both SR channel (from the UT to the UAV-BS) and RD channel (from the UAV-BS to the BS) are around 25db. But the $SINR_{SD}$ is much worse than $SINR_{RD}$ at 6th second. $SINR_{SR}$ decreased to outage condition simultaneously with $SINR_{SD}$. In Fig.8 we could see that SRD case gave instant value of $G_{goodput}$ up to 60% during the simulation. But at 6th second the gain $G_{goodput}$ is near zero.

In Fig.9 we present instant goodput values for another simulation run. In all simulated points SRD case demonstrates steady gain. For example, at 9th second $Goodput_{SD}$≈33 Mbps and $Goodput_{SRD}$≈100Mbps.

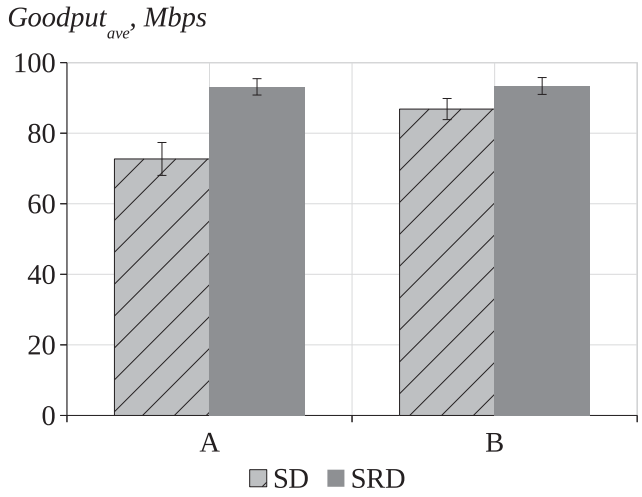

Fig. 10. Average goodput for SRD and SD cases: a) A=300 meters, $\rho_{block}=0.04$, relay position (150,150,10); *b) A=1000 meters,* $\rho_{block}=0.004$, relay position (500,500,10).

We calculated average values for goodput during 50 simulation runs. In figure 10 average goodput for transmission with the UAV-BS (SRD) and without it (SD) are presented. The UAV-BS is located in the middle of the area. On the left side of the figure high blockage is considered ($\rho_{block}=0.04$, A=300 m) and the gain is around 30%. On the right side of the figure the blockage is low ($\rho_{block}=0.004$, A=1000 meters), the average goodput is about 95 Mbps for SRD case and 85 Mbps for SD case, and the gain $G_{goodput}$ is about 7.5%.

VI. Conclusion

In this paper we estimated the applicability of UAV-assisted mmWave system in crowded area with help of NS-3 simulation tool. Our measurements show that the transmission using UAV-BS (SRD case) is more effective than the transmission without it (SD case). SRD case showed goodput gain more than 80% for blocker density of 0.1 blocker/m^2. We also measured the gain for values of side A from 100 to 1000 meters. For all measured points SRD case was better than SD case in average goodput metric due to frequent outages of mmWave link between the UT and the BS.

System level simulations are vital to estimate the efficiency of new relaying and coding techniques in emerging 5G networks. New analytical models are required to make end-to-end simulation of UAV-assisted mmWave systems more realistic and versatile.

Acknowledgment

The reported study was funded by RFBR according to the research project № 18-37-00218 mol_a.

References

[1] 3GPP, “TR 38.913, Study on Scenarios and Requirements for Next Generation Access Technologies, V14.1.0,” 2017.

[2] F. Khan and Z. Pi, “An introduction to millimeter-wave mobile broadband systems,” IEEE Commun. Mag., vol. 49, no. 6, pp. 101 – 107, Jun. 2011.

[3] T. S. Rappaport, S. Sun, R. Mayzus, H. Zhao, Y. Azar, K. Wang, G. N. Wong, J. K. Schulz, M. Samimi, and F. Gutierrez, “Millimeter Wave Mobile Communications for 5G Cellular: It Will Work!” IEEE Access, vol. 1, pp. 335–349, May 2013.

[4] S. Rangan, T. S. Rappaport, and E. Erkip, “Millimeter-wave cellular wireless networks: Potentials and challenges,” Proc. IEEE, vol. 102, no. 3, pp. 366–385, Mar. 2014.

[5] T. S. Rappaport, R. W. Heath Jr., R. C. Daniels, and J. N. Murdock, *Millimeter Wave Wireless Communications*. Pearson Education, 2014.

[6] M. Zhang, M. Mezzavilla, R. Ford, S. Rangan, S. Panwar, E. Mellios, D. Kong, A. Nix, and M. Zorzi, “Transport layer performance in 5G mmWave cellular,” in IEEE Conference on Computer Communications Workshops (INFOCOM WKSHPS), April 2016, pp. 730–735.

[7] J. S. Lu, D. Steinbach, P. Cabrol, and P. Pietraski, “Modeling human blockers in millimeter wave radio links,” ZTE Communications, vol. 10, no. 4, pp. 23–28, Dec. 2012.

[8] M. Polese, M. Giordani, M. Mezzavilla, S. Rangan, and M. Zorzi,“Improved handover through dual connectivity in 5g mmwave mobile networks,” IEEE Journal on Selected Areas in Communications, vol. 35, no. 9, pp. 2069–2084, Sept 2017.

[9] R. Ford, A. Sridharan, R. Margolies, R. Jana, and S. Rangan, “Provisioning Low Latency, Resilient Mobile Edge Clouds for 5G,” in IEEE Conference on Computer Communications Workshops (INFOCOM WKSHPS). IEEE, 2017.

[10] M.Sneps-Sneppe, D.Namiot “On 5G Projects for Urban Railways”, *Proceeding Of The 22nd Conference Of Fruct Association*, Jyvaskyla, Finalnd, May 15-18 2018, pp. 244-249.

[11] D.S. Vasiliev, I.A. Kaysina, A. Abilov, "Performance evaluation of COPE-like Network Coding in Flying Ad Hoc Networks: Simulation-based Study", *Proceedings of 17th International Conference NEW2AN 2017 10th Conference ruSMART 2017 Third Workshop NsCC 2017*, pp. 577-586, August 28–30, 2017.

[12] 3GPP TR 36.777 V15.0.0 (2017-12) Study on Enhanced LTE Support for Aerial Vehicles (Release 15).

[13] L. Chen, Y. Huang, F. Xie, Y. Gao, L. Chu, H. He, Y. Li, F. Liang, and Y. Yuan. Mobile relay in LTE-advanced systems. IEEE Communications Magazine, 51(11):144–151, 2013.

[14] L. Kong, L. Ye, F. Wu, M. Tao, G. Chen, and A. V. Vasilakos, “Autonomous relay for millimeter-wave wireless communications,” IEEE J. Sel. Areas Commun., vol. 35, pp. 2127–2136, Sept. 2017.

[15] A. Orsino, A. Ometov, G. Fodor, D. Moltchanov, L. Militano, S. Andreev, O. N. Yilmaz, T. Tirronen, J. Torsner, G. Araniti et al., “Effects of heterogeneous mobility on D2D- and drone-assisted mission-critical MTC in 5G,” IEEE Comm. Mag., vol. 55, no. 2, pp. 79–87, 2017.

[16] I. Bor-Yaliniz and H. Yanikomeroglu, “The new frontier in ran heterogeneity: Multi-tier drone-cells,” IEEE Communications Magazine, vol. 54, no. 11, pp. 48–55, November 2016

[17] N. Rupasinghe, Y. Yapici, I. Guvenc, and Y. Kakishima, “Nonorthogonal multiple access for mmWave drones with multi-antenna transmission,” available online: arxiv.org/abs/1711.10050, 2017.

[18] M. Chen, M. Mozaffari, W. Saad, C. Yin, M. Debbah, and C. S. Hong, “Caching in the sky: Proactive deployment of cache-enabled unmanned aerial vehicles for optimized quality-of-experience,” IEEE Journal on Selected Areas in Communications, vol. 35, no. 5, pp. 1046–1061, May 2017.

[19] R. Kovalchukov, D. Moltchanov, A. Samuylov, A. Ometov, S. Andreev, Y. Koucheryavy, K. Samouylov, "Analyzing Effects of Directionality and Random Heights in Drone-based mmWave Communication," in *IEEE Transactions on Vehicular Technology*. doi: 10.1109/TVT.2018.2857215

[20] T. R. Henderson, M. Lacage, G. F. Riley, C. Dowell, and J. Kopena, “Network simulations with the ns-3 simulator,” SIGCOMM demonstration, vol. 14, no. 14, p. 527, 2008.

[21] N. Baldo, M. Miozzo, M. Requena-Esteso, and J. Nin-Guerrero, “An open source product-oriented lte network simulator based on ns-3,” in Proceedings of the 14th ACM International Conference on Modeling, Analysis and Simulation of Wireless and Mobile Systems, 2011, pp. 293–298. [Online]. Available: http://doi.acm.org/10.1145/2068897.2068948

[22] NYU WIRELESS, University of Padova, “ns-3 module for simulating mmwave-based cellular systems,” Available at https://github.com/nyuwireless/ns3-mmwave
[23] M. Zhang, M. Polese, M. Mezzavilla, S. Rangan, and M. Zorzi, “ns-3 Implementation of the 3GPP MIMO Channel Model for Frequency Spectrum Above 6 GHz,” in Proceedings of the Workshop on ns-3. New York, NY, USA: ACM, 2017, pp. 71–78. [Online]. Available: http://doi.acm.org/10.1145/3067665.3067678
[24] 3GPP.2017.TR38.900,Study on channel model for frequency spectrum above 6 GHz,V14.2.0. (2017).
[25] M. Mezzavilla, M. Zhang, M. Polese, R. Ford, S. Dutta, S. Rangan, M. Zorzi “End-to-End Simulation of 5G mmWave Networks”, IEEE Communications Surveys & Tutorials, Volume 20, Issue 3, 2018, pp. 2237-2263.